

Faults Analysis and Simulation for Interior Permanent Magnet Synchronous Motor Using Simulink@MATLAB

Tao Sun, Suk-Hee Lee, Jung-Pyo Hong, *Senior Member, IEEE*
Department of Automotive Engineering, Hanyang University, Seoul, 133-791, Korea
corleon@hanyang.ac.kr, hongjp@hanyang.ac.kr

Abstract — This paper introduces major potential faults of interior PM synchronous motor (IPMSM) and their simulation realization method based on Simulink@MATLAB. IPMSM often is operated in MTPA and flux weakening control strategies. If a fault occurs, the great current or backwash voltage may be generated and damaged the motor system. The faults of IPMSM, generally, contain single-phase open circuit, single-phase and 3-phase short circuit, uncontrolled generation, and switch-on failure of one transistor. When different fault occurs, the circuit of total system including motor and inverter also will be changed. Therefore, it is necessary to analyze and establish independent model for each kind of fault. In this paper, first, the system circuit is analyzed as different fault type. Then, the corresponding models based on Simulink@MATLAB are established. The absence of experiment results leads that the veracity of simulation results can not be verified, but the waveforms will be explained by theory analysis.

I. INTRODUCTION

In automotive filed, interior PM synchronous motor (IPMSM) has been widely used to be Integrated Stator/Generator, Electric Power Steering, and even traction of Hybrid Electric Vehicle. The IPMSM is usually controlled in the maximum torque per ampere (MTPA) method and flux weakening method. The MTPA method applies maximum current to winding in order to produce great torque. And the flux weakening method applies demagnetizing current to PM in order to raise motor speed. Once a fault happens, a great pulse current or backwash voltage may be generated, which can result in irreversibly demagnetizing action in permanent magnet, exploding in dc capacitor, or damage in transistors and motor coils [1]-[4]. Considering the functions of IPMSM in automobile, the safe operation of IPMSM becomes much important as well as good performance.

In order to diagnose various potential faults and thereby optimize design or enhance protection, the fault results prediction is very important. Unfortunately, it is difficult, expensive and dangerous to test the faults, particularly for the initial design process or high power machines. Thus, the proper computer-aided simulation model for post-fault results prediction becomes much valuable and meaningful. However, so far, the motor simulation models given by most commercial softwares are only suitable for normal operation. Although the power electronics circuit simulation softwares such as PSPICE, PSCAD, PSIM and Simpower of MATLAB give a chance to

simulate motor in physical model [7], it is only available to surface-mounted PM synchronous motor. There is no inductance module which can simulate the sinusoidally varying self- and mutual-inductance of IPMSM in these circuit simulation softwares. In addition, it has to be considered that these softwares need much computation time because of the convergence calculation core [5]-[6].

Considering the flexibility and popularity, this paper presents a series of models to simulate various potential IPMSM faults in Simulink@MATLAB. First, the main potential faults are introduced and classified. Then they will be analyzed according to the post-fault circuits. Next, the simulation methods are explained in voltage equations and switch signals. Depending on the mathematic and logic analysis results, the motor drive system including controller, inverter, and motor are established. The absence of experiment results leads that the veracity of simulation can not be verified, but the waveforms will be explained by theory analysis.

II. INTRODUCTION OF IPMSM FAULTS

An equivalent circuit of the general IPMSM drive system is shown in Fig. 1. It consists of a full-bridge inverter, 3-phase wye connection windings and a controller. The potential faults may occur under many cases. However, with considering the damage level and occurring possibility [1]-[4], the following cases shown in Table I will be analyzed in this paper. Although they happen in different parts and reasons, they all can be classified to five kinds of faults as shown in Table I.

TABLE I
THE POTENTIAL FAULTS AND CLASSIFICATION

Fault Reason	Classification
Switch-on failure of both transistors on a leg	Single-phase open circuit
Break of one motor phase	
Switch-off failure of one transistor	Single-phase short circuit
Ground of one motor phase	
DC supply short circuit	3-phase short circuit
Ground of motor phases	
Switch-on failure of all transistors	Uncontrolled Generation
Switch-on failure of one transistor	-

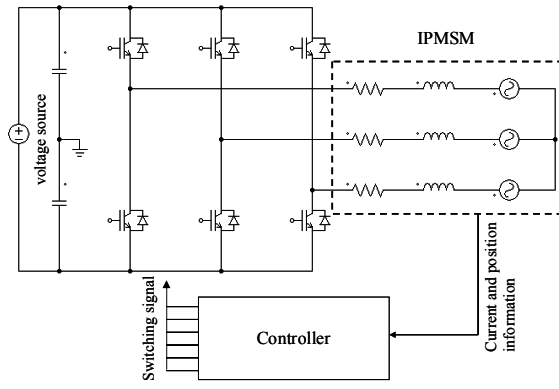


Fig. 1 Equivalent circuit of an IPMSM drive system.

III. ANALYSIS MODEL

The faultless 3-phase IPMSM generally is expressed as dq-equivalent model, the corresponding state-space equations are,

$$\begin{bmatrix} \dot{v}_d \\ \dot{v}_q \end{bmatrix} = \begin{bmatrix} R_a + pL_d & \omega L_q \\ \omega L_d & R_a + pL_q \end{bmatrix} \begin{bmatrix} i_d \\ i_q \end{bmatrix} + \begin{bmatrix} 0 \\ \omega \psi_a \end{bmatrix} \quad (1)$$

$$T = P \left[\psi_a i_d + (L_d - L_q) i_d i_q \right] \quad (2)$$

where L_d and L_q are d- and q- axis inductance, ψ_a is flux linkage of PM, R_a is phase resistance of armature winding, and P is pole-pair number.

The motor analyzed in this paper is a 12KW soft-type IPMSM which is used in a parallel-type HEV traction system. The specification of this motor is shown in Table II. The low input voltage can show the more typical post-fault characteristics [4].

TABLE II
SPECIFICATIONS OF IPMSM

Parameters	Values	
DC link Voltage	130	V
Rated phase current	190	A
d-axis inductance	0.12	mH
q-axis inductance	0.23	mH
Phase resistance	11	mΩ
Flux linkage of PM	0.03	Wb
Moment of inertial	0.0375	Kg m ²
Number of pole pair	8	-

IV. FAULT ANALYSIS IN CIRCUIT

A. Single-phase Open Circuit

The single-phase open circuit may be caused by switch-on failure of both transistors of a same leg in inverter, or a rupture between one phase winding terminal and periphery supply as shown in Fig. 2. In this case, the motor in fact is operated by the rest 2 phases, because no current flows in the fault phase winding. This asymmetrical structure is not suit for abc-dq tra-

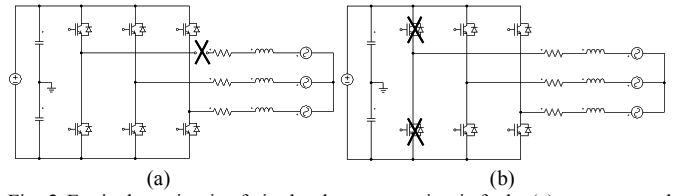


Fig. 2 Equivalent circuit of single-phase open circuit fault: (a) rupture on the terminal; (b) switch-on failure of both transistors on the same leg.

nsformation. Hence, the mathematic motor model should be modified for simulation.

The authors of [2] proposed a modified mathematical model for this condition. The key point is the absent of current in fault phase (phase a is assumed as fault phase here). Hence, the d- and q-axis currents actually are produced by the rest normal phases totally. According to dq-αβ transform, a equation only including α-axis voltage and d- and q-axis voltage variables is established.

$$\begin{aligned} v_\alpha &= -\sin \theta v_q + \cos \theta v_d \\ &= -R_a i_q \sin \theta - L_q \sin \theta \frac{di_q}{dt} - \omega \psi_a \sin \theta - \omega L_d i_d \sin \theta \\ &\quad + R_a i_d \cos \theta + L_d \frac{di_d}{dt} \cos \theta - \omega L_q i_q \cos \theta \end{aligned} \quad (3)$$

It is obvious that this is a singularity equation due to the existence of trigonometric functions. Thanks to the null phase a current, the other simultaneous equation may be obtained as,

$$i_\beta = i_q \cos \theta + i_d \sin \theta = i_a = 0 \quad (4)$$

On the other hand, the available legs of inverter become 2. Assume the controller does not reflect to the open circuit fault, and keep switching each phase every 120° electrical angle. In this paper, the SVPWM current control strategy is considered. And in this strategy, the terminal voltage of each normal phase is shown in Table III. It can be seen that the phase b and c voltages are null when their switch state are the same.

TABLE III
SWITCH SIGNAL AND TERMINAL VOLTAGE

Switch Signal	V _b	V _c
001	-V _{dc} /2	V _{dc} /2
010	V _{dc} /2	-V _{dc} /2
011	0	0
100	0	0
101	-V _{dc} /2	V _{dc} /2
110	V _{dc} /2	-V _{dc} /2
111	0	0
000	0	0

* 1 and 0 means the upper and the lower transistor is switch-on, respectively. The order of switch signals is phase a, b and c.

B. Single-phase Short Circuit

A transistor cannot switch off, which results the complementary one is switched off by a transistor protection circuit. The other potential reason is a phase terminal rupture

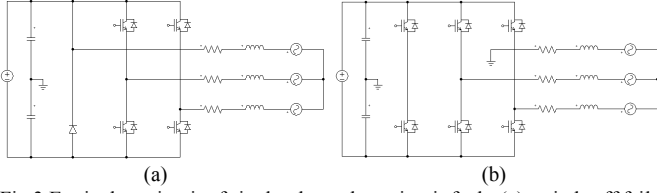


Fig.3 Equivalent circuit of single-phase short circuit fault: (a) switch-off failure of a transistor; (b) ground of one phase terminal.

TABLE IV
SWITCH SIGNAL, TERMINAL VOLTAGE, AND PHASE VOLTAGE

Switch signal	V_{ao}	V_{bo}	V_{co}	V_{an}	V_{bn}	V_{cn}
000	$V_{dc}/2$	$-V_{dc}/2$	$-V_{dc}/2$	$V_{dc}/3$	$-2V_{dc}/3$	$-2V_{dc}/3$
001	$V_{dc}/2$	$-V_{dc}/2$	$V_{dc}/2$	$V_{dc}/3$	$-2V_{dc}/3$	$V_{dc}/3$
010	$V_{dc}/2$	$V_{dc}/2$	$-V_{dc}/2$	$V_{dc}/3$	$V_{dc}/3$	$-2V_{dc}/3$
011	0	0	0	0	0	0
100	$V_{dc}/2$	$-V_{dc}/2$	$-V_{dc}/2$	$V_{dc}/3$	$-2V_{dc}/3$	$-2V_{dc}/3$
101	$V_{dc}/2$	$-V_{dc}/2$	$V_{dc}/2$	$V_{dc}/3$	$-2V_{dc}/3$	$V_{dc}/3$
110	$V_{dc}/2$	$V_{dc}/2$	$-V_{dc}/2$	$V_{dc}/3$	$V_{dc}/3$	$-2V_{dc}/3$
111	0	0	0	0	0	0

* the v_{x0} ($x=a, b$ and c) is terminal voltage of corresponding phase; the v_{xn} is the phase voltage from the terminal to neutral point of windings.

and ground as shown in Fig. 3. These two reasons will generate two different results because the terminal voltages of the fault phase are different, the former is $V_{dc}/2$, and the latter is 0 (assume the upper transistor of phase a is permanently switch-on here). For a faultless system, the 0 sequence component in abc-dq0 transformation could be ignored because its voltage is 0.

$$v_0 = \frac{1}{3}(v_a + v_b + v_c) = 0 \quad (5)$$

However, in the case of single-phase short circuit fault, the v_0 is no longer 0. Thus, the 0 sequence component voltage equation should be considered in the simulation of this case.

Unlike the case of single-phase open circuit fault, the dq-model of IPMSM is still available to this fault because the existence of Back-EMF and phase current. The Back-EMF has same frequency with the other normal phase Back-EMFs, which means the phase impedance is the same to those of faultless phases. In addition, because the 3 phases still share a same neutral voltage, as long as the switch signals are known, the each phase voltage can be obtained.

It has to be paid attention that the terminal voltage of phase a is not always $V_{dc}/2$ in the case of this transistor fault. When the rest normal phases simultaneously are turned to the same side with fault switch, the 3-phase windings get symmetrical and the terminal voltage of each phase is 0. This state is same to the 3-phase short circuit fault which will be introduced later. The relationship of switch signal, terminal voltage, and phase voltage are listed in Table IV.

C. 3-phase Short Circuit

As shown in Fig. 4, 3-phase short circuit fault possibly

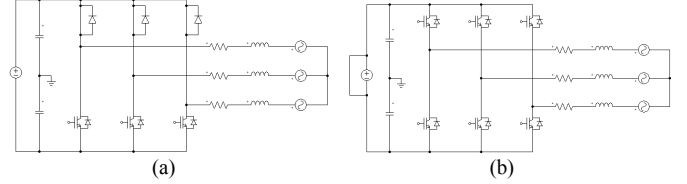


Fig.4 Equivalent circuit of 3-phase short circuit fault: (a) 3 switch-on transistors on the same side; (b) short circuit of dc link voltage source.

happens when 3 legs of inverter are switched to the same side simultaneously, the dc link voltage is short, or the 3-phase terminals ground. 3-phase short circuit also is called symmetrical short circuit because the balance phase voltage, current and impedance remain. Therefore, the mathematical model does not need to modify. It can be realized by switching 3-phase terminal voltages to 0 when the fault starts.

D. Uncontrolled Generation Fault

At over-base speed, the peak value of line-to-line Back-EMF could beyond the dc-link voltage. If there is no flux weakening control, this condition is impossible to happen in motoring mode of IPMSM. However, the flux weakening control applies a more demagnetizing d-axis current to the PM, which weakens the d-axis magnetic field and hence limits the line-to-line voltage to dc link voltage value. Once the flux weakening control suddenly disappears, the great line-to-line Back-EMF immediately becomes a voltage source and feedback power to dc source through anti-parallel diodes. This fault usually is caused by the controller problem, such as damage of DSP or position sensor, and accidental shutdown of controller power source in high-speed operation state.

In this case, the equivalent circuit of inverter becomes a 3-bridge rectifier and the Back-EMFs are the voltage source. According to the principle of rectifier, the relationship of the phase terminal voltage, line-to-line Back-EMF and phase current is obtained. There are two cases for this state, one is discontinuous phase current, and the other is continuous phase current.

For phase a (the other two are the same to it), when $V_{dc} > E_{ab}$ (or $-V_{dc} < -E_{ab}$), and no current flows in this phase winding, the phase voltage is float and uncertain. Here, the 2-phase model which is presented for solving the single-phase open circuit fault can be employed. When $V_{dc} < E_{ab}$ (or $-V_{dc} > -E_{ab}$), a negative (or positive) current starts flow in phase a. Synchronously the upper (or lower) anti-parallel diode of phase a gets bias, and the terminal voltage is clamped to $V_{dc}/2$ (or $-V_{dc}/2$). After E_{ab} gets lower than V_{dc} , due to the flowing current in phase inductance, the diode is going on bias. If the line-to-line Back-EMF is great enough, before phase current vanishes, $-V_{dc} > -E_{ab}$ (or $V_{dc} < E_{ab}$) appears, which not only keep the diode bias, but also increase the phase current. If the next $-V_{dc} > -E_{ac}$ (or $V_{dc} < E_{ac}$) can appear before the phase current produced by E_{ca} vanishes, the phase current will be continuous, otherwise be discontinuous.

E. Switch-on Failure of one transistor

Besides permanent switching on, the transistor also possibly

permanently switches off because of the absence of gating signal. In this case, the transistor protection circuit does not work. Hence the other one on the same leg still works with control signal. In the normal case, the freewheeling effect of anti-parallel diodes usually can be ignored in SVPWM current control simulation, if the inverter loss is not focused on. However, this permanent switch-off fault results that the diode has enough time to freewheeling in one switching period. Its bias will decide the phase voltage of all 3 phases.

The bias of diode not only has relationship with switch signals of transistors, but also current flowing in the fault phase winding. Assume the upper transistor of phase a fails to switch on. When the normal transistor on the fault leg is switch-off and current flows in positive direction in the fault phase, the anti-parallel of normal transistor will get bias. Inversely, if the current flows in negative direction, the anti-parallel diode of the fault transistor will get bias. Table V gives this relationship of switch signal, current state and corresponding terminal voltage. It should be paid attention that the post-fault circuit could be same to the single-phase open circuit when the fault phase current is null and normal transistor is switch-off.

TABLE V
SWITCH SIGNAL, FAULT PHASE CURRENT, AND PHASE VOLTAGE

Switch signal	i_a	V_{ao}	V_{bo}	V_{co}
000	-	0	0	0
001	-	$-V_{dc}/2$	$-V_{dc}/2$	$V_{dc}/2$
010	-	$-V_{dc}/2$	$-V_{dc}/2$	$V_{dc}/2$
011	-	$-V_{dc}/2$	$V_{dc}/2$	$V_{dc}/2$
100	$i_a < 0$	$V_{dc}/2$	$-V_{dc}/2$	$-V_{dc}/2$
	$i_a > 0$	0	0	0
101	$i_a < 0$	$V_{dc}/2$	$-V_{dc}/2$	$V_{dc}/2$
	$i_a > 0$	$-V_{dc}/2$	$-V_{dc}/2$	$V_{dc}/2$
110	$i_a < 0$	$V_{dc}/2$	$V_{dc}/2$	$-V_{dc}/2$
	$i_a > 0$	$-V_{dc}/2$	$-V_{dc}/2$	$V_{dc}/2$
111	$i_a < 0$	0	0	0
	$i_a > 0$	$-V_{dc}/2$	$V_{dc}/2$	$V_{dc}/2$

V. SIMULATION IN SIMULINK/MATLAB

Depending on the analysis of post-fault circuit, the IPMSM fault simulation is constructed with mathematic function blocks of Simulink@MATLAB. The system consists of controller module, Park's transformation module, SVPWM module, inverter module, IPMSM module, and mechanical output module.

A. Controller Module

Using proportional and integral (PI) calculation, the controller generates q-axis current reference via speed reference. And then, according to the operation speed, the MTPA method and flux weakening method will be used to calculate d-axis current reference. The calculated reference d- and q-axis currents then are compared with feedback of the d- and q-axis currents. The errors are dealt with PI again to

generate reference d- and q-axis voltages. The equations of MTPA method and flux weakening method employed in this paper are (6) and (7), respectively [8].

$$i_d = \frac{\psi_a}{2(L_q - L_d)} - \sqrt{\frac{\psi_a}{4(L_q - L_d)^2} + i_q^2} \quad (6)$$

$$i_d = \frac{-\psi_a + \sqrt{\left(\frac{V_{om}}{\omega}\right)^2 - (L_q i_q)^2}}{L_d} \quad (7)$$

As the assumption before, the controller does not reflect to the fault. It hence will be applied in any fault model.

B. Inverter Module

The inverter module receives the switch signals of SVPWM module, and converts them to terminal voltage of each phase. Based on Table III, IV, and V, the relationship of switch signals and terminal voltage is modified as different fault. The inverter module in single-phase short circuit fault and one phase rectifier module in uncontrolled generation fault simulation are shown in Fig. 5 and 6 as examples.

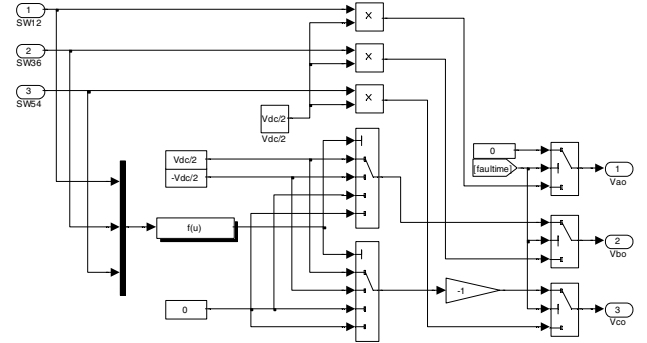


Fig. 5 Inverter module using in single-short circuit fault simulation

where the function block with shadow receives switch signals and converts them to selection signals. The next selection block will select input according to these signals. The signal routing block named "faulttime" is a fault switch signal which is used to swap normal simulation and fault simulation.

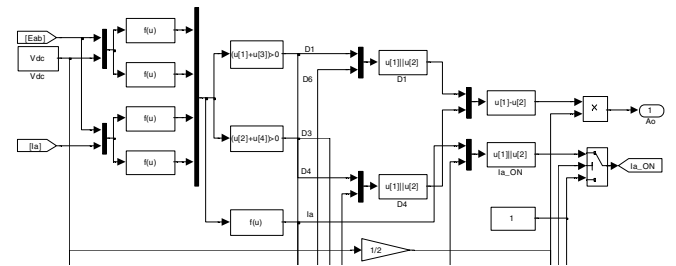


Fig. 6 One rectifier module using in uncontrolled generation fault simulation

In Fig. 6, the module first compares the line-to-line Back-

EMF and dc link voltage and judges the current flowing direction. The results decide which diode gets bias and motor mode (3-phase or 2-phase).

C. Motor Module

There are 2-phase normal motor module and 2-phase fault motor module. Based on the equation in [2], the 2-phase fault motor module is established as shown in Fig. 7. As mentioned before, this model will be used in single-phase open circuit fault, uncontrolled generation fault and switch-on failure of one transistor fault simulation. Its input variables are the terminal voltage of phase b and c, and output variables are d- and q-axis currents which are the same to the normal motor module. Therefore it can be parallel connected with normal motor module. When the fault occurs, the outputs are swapped from normal module to fault model.

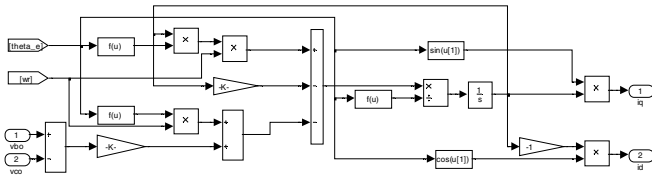


Fig. 7 2-phase motor module using in single-phase open circuit fault, uncontrolled generation circuit fault and switch-on failure of one transistor fault simulation

VI. SIMULATION RESULTS AND DISCUSSION

After import the parameters listed in Table I, the five kinds of faults are implemented. The faults are started at 1.5 s, and the reference speed is given to 3 times of base-speed (3600rpm), and 80% of maximum torque in that speed (23Nm). Especially, in order to enhance the post-fault phenomena, the simulation speed of uncontrolled generation fault is set at 5500 rpm. The results of five faults, including 3-phase current, d- and q-axis current, speed and electromagnetic torque, are shown in Fig. 8, Fig. 9, Fig. 10, Fig. 11, and Fig. 12 as the order in Table I, respectively.

Fig. 8 (a) shows 3-phase currents since steady state to single-phase open circuit fault state. It can be seen the currents become 2 phases with 180° electrical position difference after fault happens. In Fig. 8 (b), although the mean values of the d- and q-axis currents are not varying too much, but the great pulse of d-axis current is a potential danger to irreversibly demagnetize the PM. On the other hand, in Fig. 8 (c) and (d), the post-fault mean electromagnetic torque is almost zero and hence cannot maintain the pre-fault speed, which justify the constant dc link voltage.

In fig. 9 (a), the current of fault phase gets dominantly positive after 1.5 s, and the polarities of other 2-phase currents are negative. This accords with the wye connection of 3-phase windings, and the sum of 3-phase currents always is zero. Due to the dominant dc component, the fault phase current is limited by the phase resistance. This analysis model has very low resistance so that the great current is produced by low voltage. Despite the high current is applied to motor, the

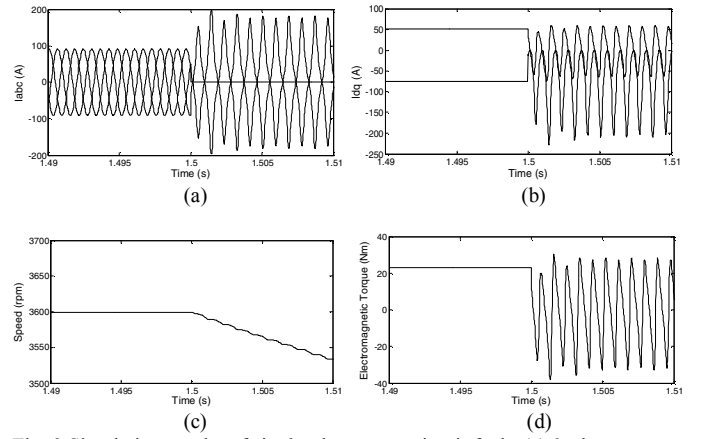


Fig. 8 Simulation results of single-phase open circuit fault: (a) 3-phase current; (b) d- and q-axis current; (c) speed; (d) electromagnetic torque.

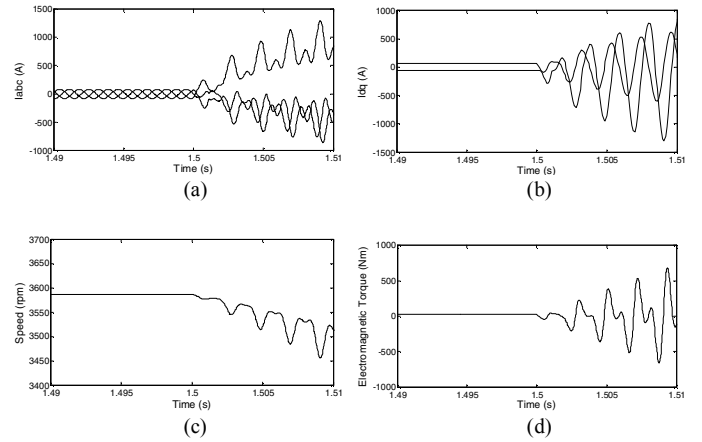


Fig. 9 Simulation results of single-phase short circuit fault: (a) 3-phase current; (b) d- and q-axis current; (c) speed; (d) electromagnetic torque.

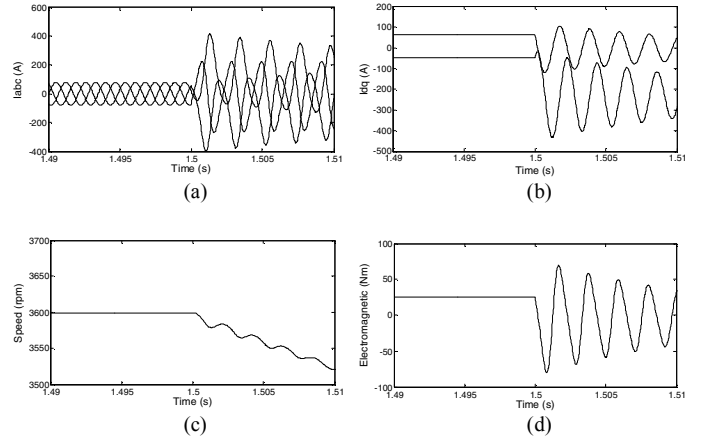


Fig. 10 Simulation results of 3-phase short circuit fault: (a) 3-phase current; (b) d- and q-axis current; (c) speed; (d) electromagnetic torque.

average of generated torque as shown in Fig. 9 (d) is zero. Due to the positive and negative great torque pulse, the speed does not reduce rapidly. Compared with the other post-fault results, the single-short circuit is the most dangerous fault. The huge short circuit current not only is possible to lead to irreversibly demagnetizing of PM, but also could burn the armature coil.

The current waveforms shown in Fig.10 (a) is in a transient

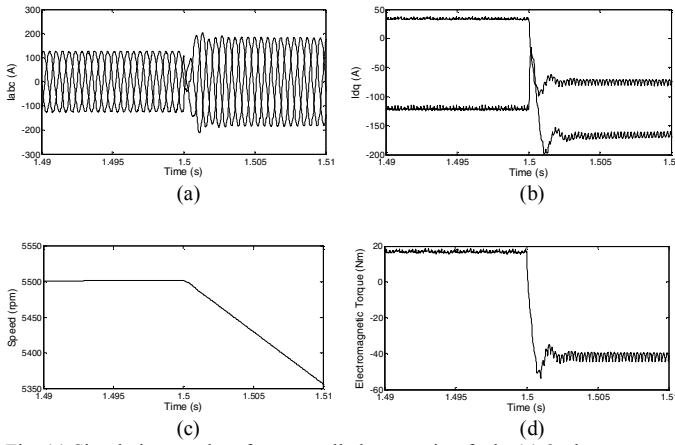


Fig. 11 Simulation results of uncontrolled generation fault: (a) 3-phase current; (b) d- and q-axis current; (c) speed; (d) electromagnetic torque.

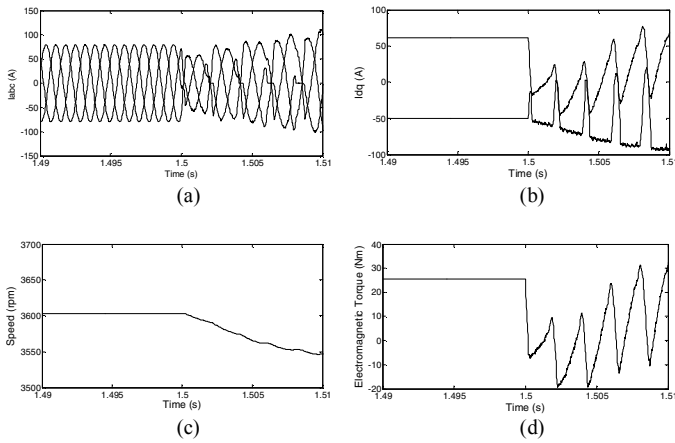


Fig. 12 Simulation results of switch-on failure of one transistor fault: (a) 3-phase current; (b) d- and q-axis current; (c) speed; (d) electromagnetic torque.

state. Although there is no voltage applies each phase winding, the transient currents achieve great magnitude. This transient state exists in beginning of any 3-phase AC circuit, which is because of the superposition of 3-phase currents in wye connected windings. Hence, it is necessary to avoid forming this uncontrollable 3-phase AC circuit. Since no input power to this system, the speed and torque tends to zero.

In Fig. 11 (a), the post-fault current has been higher than the rated current. Therefore, it is suggested that the analysis model should reduce PM volume and increase salient ratio to maintain the output power by reluctance torque. In addition, it is obvious that a phase shift occurs from fault starting. That accords with the difference of polarity in motor and generator. In Fig. 11 (d), the torque direction instantaneously reverses after fault occurs, which is because the energy source becomes Back-EMF rather than dc link voltage.

In Fig. 12 (a), it can be seen that the dominant component of phase a current is the minus part of a sinusoidal waveform. The minor positive part is due to the positive $V_{dc}/2$ applied by bias diode of fault transistor. Therefore, in order to satisfy the KCL, the rest normal currents have more positive component. This phenomenon appears as switch period. That is why the d- and q-axis current have discrete pulses. It is observe that the speed

does not decrease rapidly, because the rest five transistors are still able to respond and satisfy the command of controller. Due to the higher post-fault current, only low torque can be maintained. In practice, once the higher current is over the rated current too much, the system will be damaged. On the other hand, the great ripple also can not be ignored. It will lead to strong noise and vibration which possibly is not suitable for the requirements of environment and production.

VII. CONCLUSION

This paper analyzed the potential faults of IPMSM in equivalent system circuit. The post-fault equations, switching schemes and terminal voltages are proposed. According to the mathematic and logic analysis results, a series of dynamic simulations for these faults are established in Simulink@MATLAB. Especially, the constructions of key modules have been shown in the paper. Finally, according to the proposed simulation models, the five faults including single-phase open circuit, single-phase short circuit, 3-phase short circuit, uncontrolled generation and switch-on failure of one transistor are implemented successfully. Although the test results are absent, the validity of these simulation methods has been explained and analyzed depending on the result waveforms.

REFERENCES

- [1] N. Bianchi, S. Bolognani, and M. Zigliotto, "Analysis of PM synchronous motor drive failures during flux weakening operation," *Power Electron. Specialists Conf.*, vol. 2, Jun. 1966, pp. 1542-1548.
- [2] B. A. Welchko, T. M. Jahns, and S. Hiti, "IPM synchronous machine drive response to a single-phase open circuit fault," *IEEE Trans. Power Electronics*, vol. 17, pp.764 – 771, Sept. 2002.
- [3] B. A. Welchko, T. M. Jahns, Wen.L. Soong, and James M. Nagashima, "IPM synchronous machine drive response to symmetrical and asymmetrical short circuit faults," *IEEE Trans. Energy Conversion*, vol. 18, pp. 291-298, Jun. 2003.
- [4] Thomas M. Jahns and Vahe Caliskan, "Uncontrolled generator operation of interior PM synchronous machines following high-speed inverter shutdown," *IEEE Trans. on Industrial Applications*, vol. 35, no. 6, pp. 1347-1357, Nov./Dec. 1999.
- [5] B. K. Lee and M. Ehsani, "A simplified functional model for 3-phase voltage-source inverter using switching function concept," *IEEE Trans. on Industrial Electronics*, vol. 48, no. 2, pp. 309-321, April 2001.
- [6] Wonbok Hong, Wootaik Lee, and Byoungkuk Lee, "Dynamic simulation of brushless DC motor drives considering phase commutation for automotive applications," in *Proc. IEEE. IEMDC'07*, vol. 2, pp. 1377-1383, May. 2007
- [7] A.K. Adnanes, R. Nilssen, and R.O. Rad, "Power feed-back during controller failure in inverter fed permanent magnet synchronous motor drives with flux weakening," in *Proc. IEEE PESC'92*, Jun./Jul, 1992, vol. 2, pp. 958-963
- [8] S. Morimoto, M. Sanada, and Y. Takeda, "Effects and compensation of magnetic saturation in flux-weakening controlled permanent magnet synchronous motor drives," *IEEE Trans. on Industrial Applications*, vol. 30, no. 6, pp. 1632, Nov./Dec. 1994.



International Conference on Electrical Machines and Systems 2007

October 8 ~ 11, Seoul Olympic Parktel, Seoul, Korea



Copyright and Reprint Permission : Papers are permitted with credit to the source. Libraries are permitted to photocopy beyond the limit of Korea copyright law. Other copying, reprint or reproduction requests should be addressed to KIEE, Room 901, Science & Technology Building, 635-4, Yucksam-Dong, Kangnam-Ku, Seoul 135-703 Korea. Copyright © 2007 by The Korean Institute of Electrical Engineers.

Information about how to order the publication :

KIEE (The Korean Institute of Electrical Engineers)
Room 901, Science & Technology Building, 635-4, Yucksam-Dong, Kangnam-Ku, Seoul
135-703 Korea

Tel: +82-2-553-0151 Fax: + 82-2-566-9957 E-mail: kiee@kiee.or.kr

01. Home



02. Session List



03. Authors' Index



04. Search



Organized by



KIEE(The Korean Institute of Electrical Engineers)

Co-organized by



CES(China Electrotechnical Society)



IEEJ(The Institute of Electrical Engineers of Japan)

Technical Co-sponsor



IEEE Industry Application Society












IEEE Catalog Number : 07EX1815C

ISBN Number : 978-89-86510-07-2

Vendor : Prof. Guee Soo Cha

Tel : +82-41-530-1334 Fax : +82-41-530-1548

E-mail : gschoa@sch.ac.kr

· PMP-27	Faults Analysis and Simulation for Interior Permanent Magnet Synchronous Motor Using Simulink@MATLAB Tao Sun, Suk-Hee Lee, Jung-Pyo Hong	
· PMP-28	Effect of Rotor Pole Arc Variation on the Performance of Flux Reversal Motor Pranshu Upadhyay, N. K. Sheth, K. R. Rajagopal	
· PMP-29	New Proposal of PM-Less Super-High-Speed Blower Motor Yuta Niwa, Yuji Akiyama, Shinya Manome, Keita Miyazawa	
· PMP-30	Optimal Design of Electro-Permanent Magnet Lifter Using Improved Niching Genetic Algorithm Bum-Joo Lee, Sang-Yeop Kwak, Jang-Ho Seo, Sang-Yub Lee, Hyun-Kyo Jung	
· PMP-31	A Study on Low-Cost Sensorless Drive of Brushless DC Motor for Compressor Using Random PWM Seung-gun Lee, Dae-kyong Kim, Duck-shick Shin, Byung-taek Kim, Byung-il Kwon, Young-cheol Lim	
· PMP-32	Starting Mode Analysis of Tubular-type Linear Generator for Free-Piston Engine with Dynamic Characteristics Young-wook Kim, Jaewon Lim, Ho-Yong Choi, Sun-Ki Hong, Heesoo Lim, Si-Deok Oh, Hyun-Kyo Jung	
· PMP-33	The Optimization of 60W Linear Motor Using Response Surface Methodology Do-Kwan Hong, Byung-Chul Woo, Jong-Moo Kim, Jung-Hwan Chang	
· PMP-34	Development of Multi-layer Interior Permanent Magnet Synchronous Machine for Vehicle Sang-Yub Lee, Sang-Yeop Kwak, Jang-Ho Seo, Hyun-Kyo Jung	
· PMP-35	Comparison Evaluation for Permanent Magnet Arrangements of AC Permanent Magnet Contactor Fang Shuhua, Lin Heyun, Yang Chenfeng, Liu Xiping, Guo Jian	
· PMP-36	Modeling of End-Effect in Flux-Switching Permanent Magnet Machines Z. Q. Zhu, J. T. Chen, Y. Pang, D. Howe, S. Iwasaki, R. Deodhar	
· PMP-37	Optimum Design for Eddy Current Reduction in Permanent Magnet to Prevent Irreversible Demagnetization Jae-Woo Jung, Sang-Ho Lee, Jung-Pyo Hong, Ki-Nam Kim, Hyoung-Jun Cho, Sang-Hoon Moon	
	Shape Optimization of Rotor Pole in Spoke Type Permanent Magnet Motor for Reducing Partial	